2017

Observed mode shape effects on the vortex-induced vibration of bending dominated flexible cylinders simply supported at both ends

Ersegun Deniz Gedikli
University of Rhode Island

David Chelidze
University of Rhode Island, chelidze@uri.edu

See next page for additional authors

Citation/Publisher Attribution
Gedilki, E. D., Chelidze, D., & Dahl, J. M. (2017). Observed mode shape effects on the vortex-induced vibration of bending dominated flexible cylinders simply supported at both ends. *Journal of Fluids and Structures, 81*, 399-417. doi: 10.1016/j.jfluidstructs.2018.05.010
Available at: https://doi.org/10.1016/j.jfluidstructs.2018.05.010

Observed mode shape effects on the vortex-induced vibration of bending dominated flexible cylinders

Ersegun Deniz Gedikli[a,b], David Chelidze[c], Jason M. Dahl[a,*]

[a] *Ocean Engineering, University of Rhode Island, Narragansett, RI, 02882, USA*
[b] *Sustainable Arctic Marine and Coastal Technology (SAMCoT), Centre for Research-based Innovation (CRI), Norwegian University of Science and Technology (NTNU), Trondheim 7491, Norway*
[c] *Mechanical, Industrial and Systems Engineering, University of Rhode Island, Kingston, RI, 02881, USA*

Abstract

The structural mode excitation of bending-dominated flexible cylinders undergoing vortex-induced vibrations was investigated using multivariate analysis of the excited empirical modes. The response of the bending-dominated cylinders was compared with the response of a tension-dominated cylinder using the same analysis technique. Experiments were conducted in a recirculating flow channel with a uniform free stream with Reynolds numbers between 650 and 5500. Three bending-dominated cylinders were tested with varying stiffness in the cross-flow and in-line directions of the cylinder in order to produce varying structural mode shapes associated with a fixed 2:1 (in-line:cross-flow) natural frequency ratio. A fourth cylinder with natural frequency characteristics determined through applied axial tension was also tested. The spanwise in-line and cross-flow responses of the flexible cylinders were measured through motion tracking with high-speed cameras. Global smooth-orthogonal decomposition was applied to the spatio-temporal response for mode identification. Measured responses are compared with the analytic response of a beam subjected to a uniform periodic loading. Both the analytic and experimental results show that for excitation of low mode numbers, the cylinder is unlikely to oscillate with an even mode shape in the in-line direction due to the symmetric drag loading, even when the system is tuned to have an even mode at the expected frequency of vortex shedding. In addition, no mode shape changes were observed in the in-line direction unless a mode change occurs in the cross-flow direction, implying that the in-line response is a forced response dependent on the cross-flow response. An even mode oscillation (i.e. second mode) in the in-line direction is observed to be excited in the tensioned cylinder, however this is only observed in a hysteretic response region, resulting in a pedaling mode response. The results confirm observations from previous field and laboratory experiments, while demonstrating how structural mode shape can affect vortex-induced vibrations.

Keywords: Vortex-induced vibration, Flexible cylinder, Multivariate analysis, Mode shape

1. Introduction

The vortex-induced vibration (VIV) of long, flexible structures is a complex problem due to the large number of variables that can contribute to the coupled response of the structure with the surrounding fluid (Sarpkaya, 2004). While a significant number of experimental studies have been devoted to characterizing the fundamental fluid-structure interaction for an elastically mounted rigid circular cylinder undergoing vortex-induced vibrations (Bearman, 1984; Sarpkaya, 2004; Williamson and Govardhan, 2004; Bearman, 2011), the spanwise effects of flexible structures have been more difficult to quantify due to the complexity of additional variables associated with flexible, continuous systems that are capable of multi-modal responses.

In the single degree of freedom spring-mass-dashpot model for vortex-induced vibrations, the forcing function resulting from vortex shedding may be represented as a phase shifted harmonic function to the first order approximation (Sarpkaya, 2004). Assuming a sinusoidal response to the system, one can show that the amplitude and frequency

*Corresponding author
Email address: jmdahl@uri.edu (Jason M. Dahl)

of a cylinder undergoing vortex-induced vibrations in purely cross-flow excitation are functions of the motion of the cylinder and the resulting forces acting on the cylinder in phase with the acceleration and velocity of the body. The force in phase with acceleration alters the effective mass of the system, while the fluid force in phase with velocity alters the effective damping of the system. Since these fluid force terms are functions of the motion of the body, the frequency at which the body oscillates may constantly change in time, however this frequency is often fairly constant when observed in laboratory experiments. Using integral quantities of the forces in phase with velocity and acceleration, one can consider the system to have an effective natural frequency that is dependent on the fluid force in phase with acceleration.

In contrast to a single degree of freedom system, the natural frequencies of a continuous system are not only related to the stiffness and mass of the physical structure, but also are dependent on the particular spanwise shape of the oscillating structure. For example, an infinite string contains an infinite number of natural frequencies with each frequency corresponding to a particular spanwise shape. In VIV, the relative motion of vortices shed from the structure in relation to the motion of the body determines the phasing and magnitude of forces exerted on the body, hence for a continuous structure, the particular shape of the structure oscillation must have an effect on the resulting forces exerted on the structure. If we model a continuous system undergoing VIV similar to the 1-DOF system undergoing VIV, this would imply that the mode shapes corresponding to particular natural frequencies of the structure must be excited when that natural frequency is excited (or slightly modified by the added mass). The problem with this assumption is that since the fluid forces are dependent on the body oscillation and vice versa, there is no guarantee that the resulting fluid forces will drive a motion that is consistent with the analytic structural mode shape in a vacuum.

The complexity of the flow-induced vibration of flexible cylinders is evident in the variety in the types of responses that are observed for these types of structures. For instance, the flow-induced vibration of flexible structures may undergo complex three-dimensional vibrations, experiencing traveling waves (Marcollo et al., 2011) and chaotic motions (Modarres-Sadeghi et al., 2011). Sarpkaya (2010) discusses such complexities and effects of additional VIV parameters on the dynamic response. A variety of studies on marine risers (Lie and Kaasen, 2006; Chaplin et al., 2005; Trim et al., 2005; Vandiver et al., 2005) have shown that long, flexible structures exhibit similar forcing from vortex shedding as that observed for rigid cylinders, where vortex shedding leads to an oscillating drag force with a dominant frequency that is twice the oscillating lift force frequency. The laboratory experiments conducted by Passano et al. (2010), Huera-Huarte et al. (2014) and field experiments conducted by Vandiver et al. (2005), Vandiver and Jong (1987) showed that for long flexible structures subjected to vortex-induced vibrations, it is possible to excite different modes in in-line and cross-flow directions separately, as observed from the frequency of the response and reconstructions of the spatial shape of the structure. In particular, Huera-Huarte et al. (2014) examined very low mass ratios $\sim$1, where the response frequency can vary significantly due to forcing in phase with the acceleration of the body.

In an effort to model the effects of different modal excitations in flexible cylinders, Dahl et al. (2006) investigated the effect of differing natural frequency ratios (in-line to cross-flow) on an elastically mounted rigid cylinder. The cylinder was allowed to oscillate both in cross-flow and in-line directions while the natural frequency in each direction was tuned with different values to model a long structure excited with different structural modes in each direction. These experiments demonstrated response behaviors that consisted of preferred figure-eight type motions where the cylinder moves upstream at the top and bottom of its orbital motion, which can contribute to large third harmonic forcing of the structure in the lift direction (Dahl et al., 2007). Similar studies by Srinil et al. (2013) and Kang and Jia (2013) have demonstrated similar behaviors and expanded understanding of frequency ratio effects on a rigid cylinder response for frequency ratios less than one, where tear drop shape motions may be observed with multifrequency excitation of the structure in the in-line direction. Dahl et al. (2010) observed similar behaviours for rigid cylinders at supercritical Reynolds numbers.

This paper attempts to systematically test the effects of vortex-induced vibrations on the expected modal response of a flexible body by tuning several beams to have specific frequency properties for specific structural mode shapes. The purpose of these experiments is to illustrate differences in the response of a flexible structure from an elastically-mounted rigid structure due to the spanwise excitation of the flexible structure. Comparisons are made with a bending-dominated structure and tension dominated structure, with the modal response analyzed empirically through multivariate analysis. In the experiments, three flexible cylinders were designed and tested to understand the dynamic relationship between the cylinder's structural characteristics and the modal response. Assuming that one can control the modal response of a flexible cylinder by controlling the structural characteristics (this is a significant as-

sumption since the fluid-structure interaction will inherently change these effective properties), it is possible to excite the flexible cylinder with a particular mode shape. For example, in the present experiments, a plastic beam with a particular cross-section and material characteristics was used to tune the structural mode characteristics, encouraging the cylinder to oscillate with a desired mode shape when the frequency of that particular mode shape is reached by anticipating the forcing frequency in the in-line direction to be twice the frequency in the cross-flow direction.

One may expect a cylinder to oscillate with first mode shape (half sinusoidal) when it is excited with a forcing function at the first mode frequency, and second mode shape (full sinusoid) when it is excited with the second mode frequency; however, if the flow is uniform, can even modes (asymmetric modes) in the in-line direction be truly excited? Vandiver and Jong (1987) argued that these modes would not be excited due to the distribution of the forcing function. If these even modes cannot be excited, what body motions will be observed and which frequencies will dominate the motion? This study aims to systematically understand this behavior through a set of experiments using specifically crafted model cylinders. The cylinders are placed in a uniform flow to observe the resulting response over a range of reduced velocities. The results are compared with experiments for a tension-dominated system (Gedikli and Dahl, 2017) (see Fig. 1a) in which the experimental setup is identical to the current system.

2. Methods

Experiments were conducted in a recirculating flow channel that is located at the University of Rhode Island's Narragansett Bay campus. The channel test section is made of glass featuring a downstream viewing window, allowing for visual motion tracking of the test apparatus within the test section. In the experiments, tests were conducted for flow speeds between 0.1-0.7 m/s, where free surface disturbances due to the operation of the flow channel were negligible.

Figure 1 shows the top view of the test cylinders that were mounted across the viewing walls of the flow channel. Fig.1(a) shows the tension dominated cylinder and Fig.1(b) shows the second mode excitation of a bending dominated cylinder as an example response where T represents the applied tension and U represents the flow speed. Flow is uniform moving from left to right.

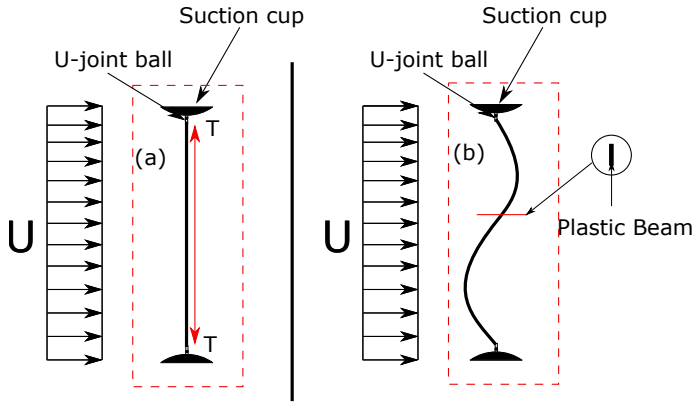

Figure 1: Schematic drawing of top view of the flow channel. Idealized in-line even mode excitation for (a) tension (see Gedikli and Dahl (2017)) and (b) bending dominated cylinder under uniform flow. T is the initial tension applied to the cylinder.

2.1. Cylinder design and experiments

Dahl et al. (2010) showed that in combined in-line and cross-flow oscillations, the in-line frequency of motion naturally adjusts to be twice the cross-flow frequency over a large range of non-dimensional flow speeds where the motion of the body can be characterized by a singular frequency in the cross-flow direction while the in-line has twice the cross-flow frequency. Using this information, structural beam characteristics in the present study were chosen such that there would be a 2:1 (in-line to cross-flow) frequency ratio between the excited structural mode shapes. This was achieved by varying the cross-sectional dimensions of a beam that was then molded inside a urethane cylinder.

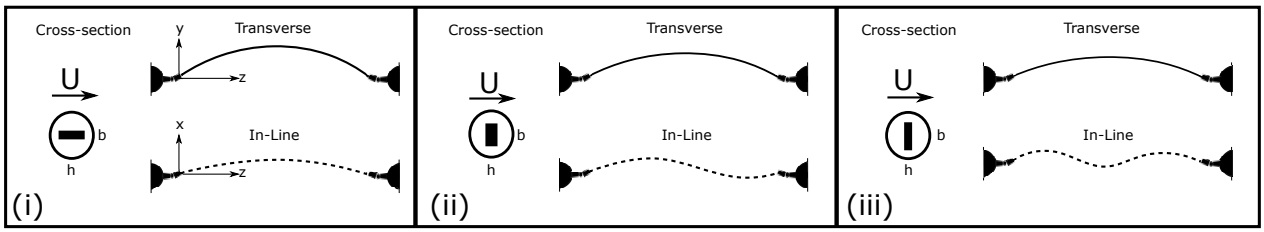

Figure 2: Idealized structural modes for the bending dominated test cylinders. Cylinders are constructed to have a frequency ratio of 2:1 between the in-line and cross-flow directions. (i) Cylinder 1: First mode in-line, first mode transverse, (ii) Cylinder 2: Second mode in-line, first mode transverse, (iii) Cylinder 3: Third mode in-line, first mode transverse.

To investigate the effects of the combined in-line and cross-flow spatial modal response, the tuned structure's in-line mode shape was varied while keeping the cross-flow structural mode constant. In the experiments, 4 cylinders were tested, where cylinder 1 was tuned to have a first mode in-line and first mode cross-flow with an in-line natural frequency twice the cross-flow natural frequency. Cylinder 2 was tuned to have a first mode shape in the cross-flow and second mode in the in-line with the in-line natural frequency twice the cross-flow natural frequency. Similarly, cylinder 3 was tuned to have a first mode shape in cross-flow and a third mode shape in in-line with an in-line natural frequency twice the cross-flow natural frequency as illustrated in Fig.2. Lastly, cylinder 4 was a tensioned cylinder made of urethene rubber with no beam inside (see Gedikli and Dahl (2017) for details of the experiment). Figure 2 illustrates the idealized mode shapes of each test cylinder with different beam cross-sections.

Beam dimensions were chosen according to a simply-supported tensioned beam with natural frequencies as:

$$f_n = \sqrt{\frac{EI\pi^2 n^4}{4ML^4} + \frac{Tn^2}{4ML^2}} \tag{1}$$

where E is the modulus of elasticity, I is the area moment of inertia, n is the mode number, M is the mass per unit length, and T is the static tension. The applied tension for cylinders 1,2 and 3 was negligible compared with the stiffness of the beams, hence the second term in Eq.1 can be neglected for those beams. The simplified natural frequency equation for cylinders 1,2 and 3 can be written as:

$$f_n = \frac{\pi n^2}{2}\sqrt{\frac{EI}{ML^4}} \tag{2}$$

where n varies depending on the desired mode number, and I varies depending on the orientation and dimensions of the beam molded inside the cylinder. The area moment of inertia in the in-line (I_x) and cross-flow (I_y) was different to achieve the desired frequency characteristics of the beam. Using Eq.3, the required beam sizes were determined for specific combinations of structural modes in a vacuum. The calculated cylinder characteristics and dimensionless parameters are shown in Table 1 for each cylinder.

$$I = \frac{ML^4}{E}\left(\frac{4f_s^2}{\pi^2 n^4}\right), \quad \text{where } I \rightarrow \quad I_x = \frac{bh^3}{12}, I_y = \frac{b^3 h}{12} \tag{3}$$

To mount the cylinder in the flow channel, a universal ball joint was attached to a suction cup on each end of the test cylinder. End-plates were mounted at the location of the u-joint in order to inhibit three-dimensional flow irregularities at the ends of the cylinder. The suction cups allowed the test cylinder to be mounted horizontally in the flow channel by mounting directly to the glass walls. The test cylinders were aligned with respect to the still water free surface using a laser. Each test cylinder was marked with $23-25$ white dots, evenly distributed with spacings of $1\ cm$ along the span. The cylinder motion was captured using two synchronized Phantom V10 high speed cameras, operating at a frame rate of $250Hz$. Motion tracking software (ProAnalyst) was used to determine the displacement of each data point in the in-line and cross-flow directions. The software works based on sub-pixel accuracy where the mean position of each data point is tracked with an error margin less than 1% in all directions. A more detailed description of the experimental setup and details of the motion tracking routine are documented in Gedikli and Dahl (2017).

Table 1: Cylinder characteristics and dimensionless parameters.

Parameter (Abbrv., Unit)	Equation	Cylinder 1	Cylinder 2	Cylinder 3	Cylinder 4
Cylinder Type	-	Bending	Bending	Bending	Tension
Cylinder Material	-	Urethene	Urethene	Urethene	Neoprene
Beam Material	-	Plastic	Plastic	Plastic	None
Diameter (D, mm)	-	6.35	6.35	6.35	6.35
Cylinder Length (L, mm)	-	250	250	250	250
In-line beam width (h, mm)	-	1.27	2	2.25	None
Cross-flow beam width (b, mm)	-	2.5	0.04	0.508	None
Initial Tension (T, N)	-	-	-	-	0.15
Blockage Ratio (BR)	T/H	1.66	1.66	1.66	1.66
Aspect Ratio (AR)	L/D	41	41	41	41
Mass Ratio (m)	$4m/(\rho\pi LD^2)$	1.1	1.05	1.02	3.7
Reynolds Number (Re)	UD/ν	1500-5500	1700-5400	1600-4700	650-3500
Sampling frequency (f_{samp}, Hz)	-	250	250	250	250
In-line natural frequency (f_{IL}, Hz)	Mode 1	34	7	1.82	3
	Mode 2	136	28	7.3	6
	Mode 3	306	63	16.4	12
Cross-flow natural frequency (f_{CF}, Hz)	Mode 1	17	14	8.2	3
	Mode 2	68	56	32.8	6
	Mode 3	153	126	73.8	12

3. Amplitude Response

Fig. 3 shows the maximum RMS amplitude response for each tested cylinder as a function of the reduced velocity. The top image shows the cross-flow RMS response amplitude over the entire cylinder span and the bottom image shows the in-line RMS response amplitude over the entire cylinder span.

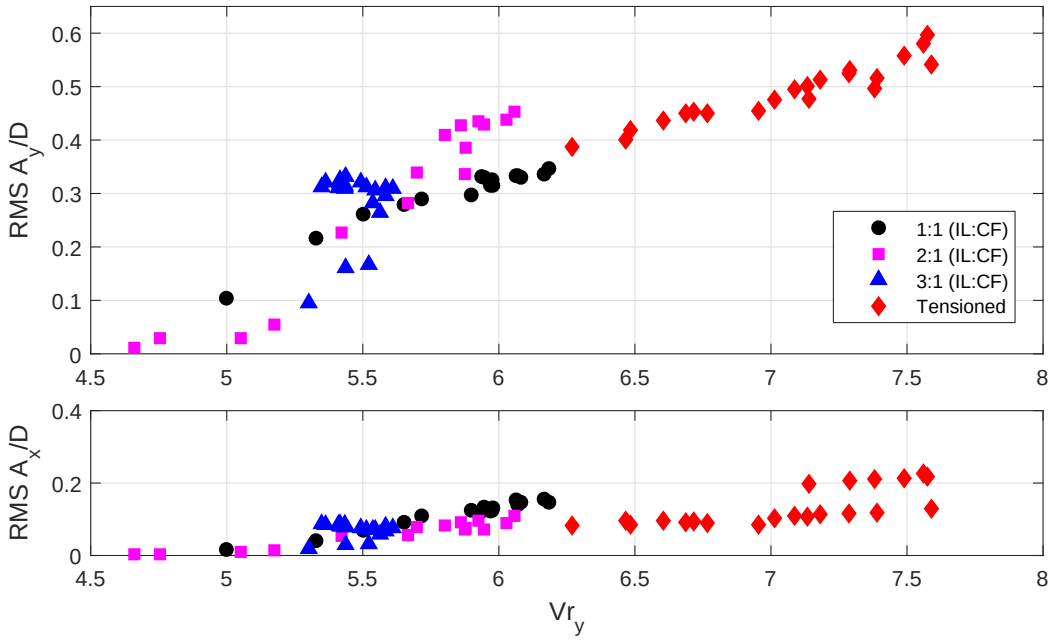

Figure 3: RMS amplitude response over the span as a function of reduced velocity. Colors indicate separate test cylinders. Black circle shows cylinder 1, purple square shows cylinder 2, blue triangle shows cylinder 3 and red diamond shows the tensioned cylinder (cylinder 4).

As seen in Fig.3, the tension dominated cylinder 4 (red diamond) was observed to have the highest cross-flow RMS amplitude response among all the cylinders tested, reaching a maximum amplitude at reduced velocity of 7.6, near the highest flow speed tested. Alternately, cylinder 1 (black circle) and cylinder 2 (purple square) reached maximum cross-flow RMS amplitude at reduced velocities of 6.3 and 6, respectively, over the same range of tested flow speeds. Although the tests were performed over a similar range of flow speeds with parameters tuned to achieve similar reduced velocities, cylinder 3 (blue triangle) was observed to oscillate in a very narrow band region between

reduced velocity values of 5.3 and 5.65. The observed maxima in the response curves typically occur at the highest flow speeds, where additional tests could not be conducted at higher speeds due to limitations of the flow channel.

The in-line amplitude responses show similar trends to the cross-flow responses where cylinders 1 and 2 have increasing amplitude responses with increasing reduced velocity. However, unlike the cross-flow response, cylinder 1 reaches a higher amplitude response in the in-line direction than cylinder 2, opposite from the observed cross-flow response. This is likely due to changes in phasing between the in-line and cross-flow responses due to the different frequency characteristics of the beams.

The response for Cylinder 3 consists of two distinct regions of clustered points in the cross-flow response, indicating two separate types of response. One region lies in between the RMS amplitudes of 0.25 and 0.35. In this region, the cylinder oscillates with 2:1 (in-line:cross-flow) frequency ratio and has a typical figure eight type of response. The second region is apparent between the RMS amplitudes of 0.1 and 0.2. In this region, the cylinder oscillates with 1:1 (in-line:cross-flow) frequency ratio, and the response motion resembles a tear drop shape. These responses are discussed in more detail in subsequent sections.

The response for Cylinder 4 also consists of two response regions, with the regions more distinct in the in-line response for reduced velocities in between 7.2 and 7.7. Unlike cylinder 3, the two response regions in the motion of cylinder 4 is due to a mode transition and change in response along the span of the cylinder. Below a nominal reduced velocity of 7.2, the cylinder oscillates with a dominant first mode in both directions, and above the nominal reduced velocity of 7.2, the dominant first mode switches to second mode in cross-flow and to some combination of second and third mode in the in-line direction. It is important to note that Cylinder 4 exhibits a hysteric response as a function of increasing or decreasing the flow speed in the flow channel, which is discussed in Gedikli and Dahl (2017).

4. Frequency Analysis

The normalized frequency response in the in-line and cross-flow directions are shown as a function of normalized reduced velocity for each cylinder in Figs. 4 and 5.

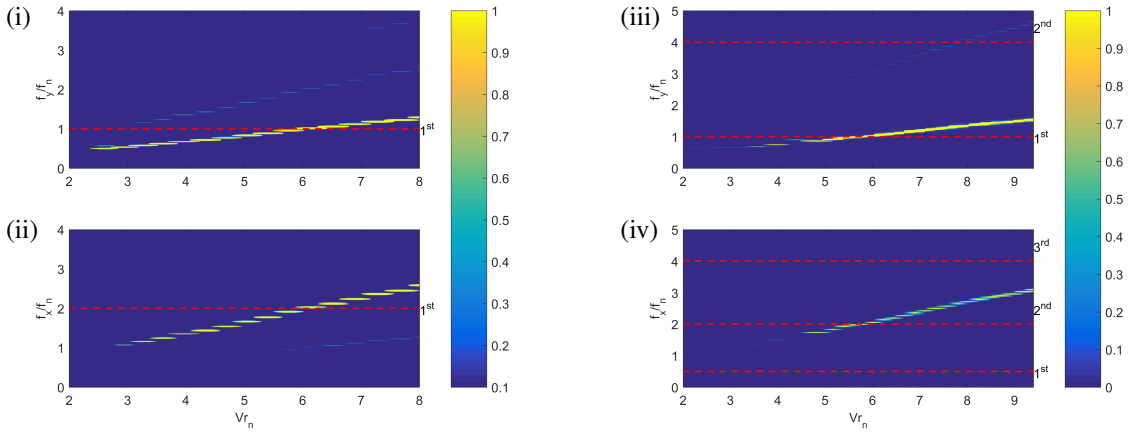

Figure 4: Frequency spectra as a function of nominal reduced velocity for cylinder 1 and cylinder 2. All spectra are normalized by the respective cylinder's fundamental frequency in the cross-flow direction. The magnitudes of the spectra are normalized by the maximum power spectral density over the range of experiments. (i) Frequency response for cylinder 1 in cross-flow. (ii) Frequency response for cylinder 1 in in-line. (iii) Frequency response for cylinder 2 in cross-flow. (iv) Frequency response for cylinder 2 in in-line. Red dashed lines indicate the structural natural frequencies in the respective directions of each individual plot. The structural mode that is associated with a particular frequency is noted on the right side of each subplot.

The left two images in Fig.4 show frequencies for cylinder 1 and the right two images in Fig. 4 show frequencies for cylinder 2 in the cross-flow and in-line directions. In the cross-flow direction, the frequency analysis shows that the dominant frequency increases with flow speed and does not level off at the natural frequency, consistent with observed responses for low mass ratio cylinders. In addition, there are higher harmonic frequency components present. In the

in-line direction, the dominant frequency is twice the frequency in the cross-flow direction for all the flow speeds tested with small lower frequency components present in the response at higher reduced velocities.

Similar to cylinder 1, the frequency content for cylinder 2 displays a 2:1 (in-line:cross-flow) dominant frequency ratio that is observed for all flow speeds tested. There is also higher harmonic frequency content present in the cross-flow direction at higher reduced velocity while higher harmonic components are not observed in the in-line direction. It should be noted that, since all frequencies in Fig. 4 are normalized by the fundamental natural frequency in cross-flow, then frequencies can be compared directly across plots, such that the in-line frequencies are typically observed to be twice the cross-flow frequency. Dotted lines indicate the structural natural frequencies that were tuned for each cylinder in order to achieve desired structural mode shapes with specific frequency combinations. For example, for cylinder 2, in the in-line direction (Fig. 4 (iv)), the lowest dotted line corresponds to a first mode in the in-line direction, but the frequency of this mode is one half the fundamental frequency in the cross-flow direction, hence $f_x/f_n = 0.5$ for this line, while the second mode for this cylinder has $f_x/f_n = 2$. For the cylinder responding with frequency content near a particular dashed line, one may expect the cylinder to take on the particular structural mode shape associated with that frequency; however, multivariate analysis of the spatial response of the cylinders will show that this is not the case, despite the clear presence of a 2:1 frequency relationship between the in-line and cross-flow directions for both of these cylinders and the observation of response frequencies that pass through different structural mode frequencies.

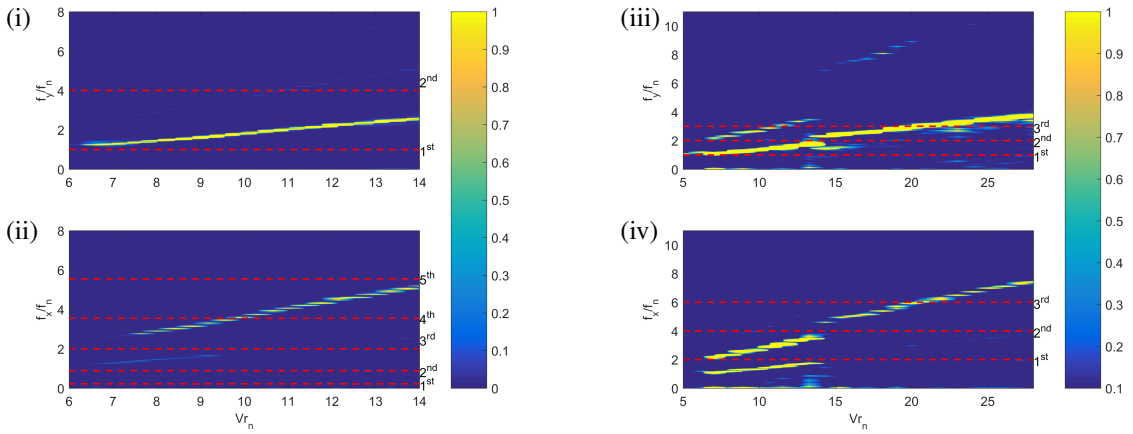

Figure 5: Frequency spectra as a function of nominal reduced velocity for cylinder 3 and cylinder 4. All spectra are normalized by the respective cylinder's fundamental frequency in the cross-flow direction. The magnitudes of the spectra are normalized by the maximum power spectral density over the range of experiments. (i) Frequency response for cylinder 3 in cross-flow. (ii) Frequency response for cylinder 3 in in-line. (iii) Frequency response for cylinder 4 in cross-flow. (iv) Frequency response for cylinder 4 in in-line. Red dashed lines indicate the structural natural frequencies in the respective directions of each individual plot. The structural mode that is associated with a particular frequency is noted on the right side of each subplot.

Figure 5 shows the cylinder 3 (left two images) and cylinder 4 (right two images) frequency content in the in-line and cross-flow directions normalized by the cross-flow fundamental natural frequency. Similar to cylinder 1 and cylinder 2, the dominant frequency for cylinder 3 in the cross-flow direction increases as the flow speed increases. In addition, there are higher harmonic frequencies present, although they are not strong in the cross-flow direction. In the in-line direction, at very low reduced velocity, the dominant frequency is equal to the frequency in cross-flow up to the nominal reduced velocity of 7.3. For higher reduced velocities, the dominant in-line frequency becomes twice the cross-flow frequency. It should be noted that cylinder 3 was designed with the intention of exciting the third structural mode shape in the in-line direction and first structural mode in the cross-flow direction. In the in-line direction, the dominant frequency is never observed to take the third in-line mode value (at two times the cross-flow first mode frequency). The system avoids oscillating at this frequency as seen in a frequency jump that occurs at nominal reduced velocity of 7.3. Instead, the system oscillates with a lower frequency in the in-line direction, then switches to a higher frequency, avoiding the structural third mode frequency altogether. This illustrates the significance of specific in-line and cross-flow mode combinations, as complex interactions between the wake and structure can significantly alter the

expected response of the system.

The two images on the right side of Fig.5 show the frequency spectra for cylinder 4 (tensioned cylinder) which is based on the displacement data from Gedikli and Dahl (2017). In contrast to the three bending dominated cylinders, cylinder 4 shows significant regions with multi-frequency content. In addition, the test range of the reduced velocities for this cylinder is much larger due to the lower natural frequencies, hence a larger region of the frequency response is shown. In particular, cylinder 4 displays first and second mode frequency components for the same nominal reduced velocities up to the nominal reduced velocity of 14, where the in-line and cross-flow excitation frequencies start to get close to the second structural mode frequencies. Above the reduced velocity value of 14, the cylinder displays different response characteristics due to a mode change in the cross-flow direction, this is accompanied by a distinct change in the excitation frequencies, where a jump occurs in the in-line direction.

4.1. Dynamic response relationship between in-line and cross-flow

In order to obtain a more complete understanding of the total cylinder response, the in-line and cross-flow spanwise response, phase angle between in-line and cross-flow along the span, center point frequencies, and center point Lissajous figures are shown for selected reduced velocities of each cylinder. The phase angle distribution was calculated using the inner product method as described in Gedikli and Dahl (2017).

4.1.1. Cylinder 1

For cylinder 1, the test cylinder was tuned to try to excite the first structural mode in both directions (in-line and cross-flow) where the first structural mode frequencies had a relation of 2:1 (in-line:cross-flow). The frequency response in Fig.4 showed that cylinder 1 vibrates near the frequency associated with the fundamental modes in both directions. Two separate flow speed cases are selected to expand on characterizing the dynamic response of the cylinder. The test case for $V_{rn} = 4.6$ is chosen for comparison as the observed response frequency lies below the structural first mode frequency and the test case for $V_{rn} = 6.8$ is chosen as the observed response frequency lies above the structural first mode frequency, as indicated with the dotted line in Fig. 4. The phase averaged spanwise response amplitude and Lissajous figures for the center points are shown in Fig. 6 for both of these cases.

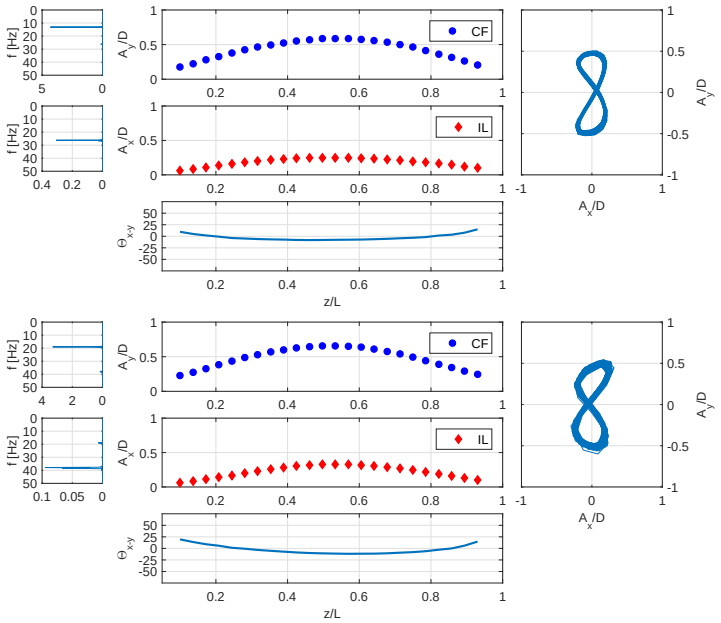

Figure 6: Spanwise response of cylinder 1, showing the frequency spectrum for the center point in cross-flow and in-line directions, the maximum spanwise response in the cross-flow and in-line directions, the computed phase between in-line and cross-flow motions, and the Lissajous figure of the center point. Top image: $Vr_n = 4.6$. Bottom image:$Vr_n = 6.8$.

As expected, the cylinder oscillates with a shape similar to a dominant first mode in both in-line and cross-flow directions. In these cases, the Lissajous figure at the cylinder center point shows a figure eight shape with a phase angle close to zero, with slight changes to the phase as one moves outwards from the center. The figure eight orbital motion of the cylinder is consistent with the type of motion observed for rigid elastically mounted cylinders Dahl et al. (2006). This is an expected observation, since the excited spanwise mode shape in the in-line direction was tuned to be the same as in the cross-flow direction in this case.

4.1.2. Cylinder 2

For cylinder 2, the test cylinder was tuned to try to excite the first structural mode shape in the cross-flow direction and the second structural mode shape in the in-line direction with a 2:1 (in-line:cross-flow) ratio between the structural mode frequencies. Based on Fig.4, the frequencies of the cylinder response lie very close to these tuned structural mode frequencies for the tested speed range. It was expected that the system would therefore oscillate with a first mode shape in the cross-flow direction and a second mode shape in the in-line direction. Test cases for $V_{rn} = 5.6$ and $V_{rn} = 8.6$ are shown as examples to demonstrate the response of cylinder 2.

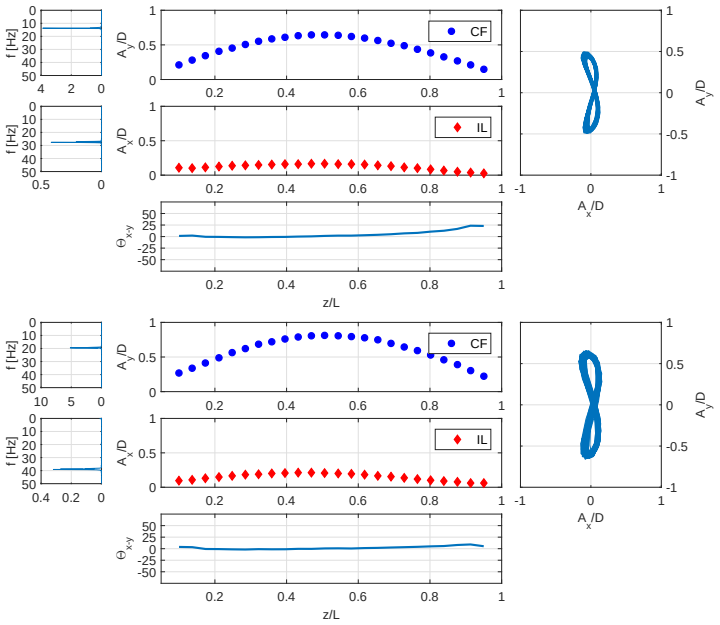

Figure 7: Spanwise response of cylinder 2, showing the frequency spectrum for the center point in cross-flow and in-line directions, the maximum spanwise response in the cross-flow and in-line directions, the computed phase between in-line and cross-flow motions, and the Lissajous figure of the center point. Top image: $Vr_n = 5.6$. Bottom image:$Vr_n = 8.6$.

Fig. 7 shows the spanwise response of cylinder 2 at $V_{rn} = 5.6$ and $V_{rn} = 8.6$ along with the Lissajous figures at the center point. At these flow speeds, a 2:1 oscillation frequency ratio is observed between in-line and cross-flow motion, as evident in the curved figure eight Lissajous figures. The phase between in-line and cross-flow motion is observed to be near zero in both cases. Of note, is that although the cylinder is excited with a first mode in the cross-flow direction as expected, the response in the in-line direction is different than anticipated. Although the frequency of the response in the in-line direction is twice the frequency of the cross-flow direction, the spanwise shape of the response in the in-line direction is similar to a half sinusoid shape, with only slight asymmetries near the end points. In these cases, the mean deflection of the cylinder due to drag has been removed, such that these responses only show the magnitude of the oscillation in the in-line direction.

This behavior was observed to be consistent for all reduced velocities tested, such that the in-line response of cylinder 2 was never observed to take on a full sinusoidal second mode shape. Since higher speeds could not be tested, it is unclear if this behavior would hold at speeds where the second mode in the cross-flow direction begins to be excited. It is important to note, however that based on this case, representing vortex-induced vibrations as a

resonant vibration occurring separately in the in-line and cross-flow directions would be incorrect, since the second structural mode shape is not excited. Instead, it appears the cylinder undergoes a forced in-line motion, which happens to occur near the second mode natural frequency, but due to the spanwise uniform loading of the cylinder in drag, the second mode shape is not excited. This observation is consistent with observations by Vandiver and Jong Vandiver and Jong (1987) where a similar behavior was observed in the field testing of a long cable in a uniform current.

4.1.3. Cylinder 3

Cylinder 3 was tuned to excite the first structural mode in the cross-flow direction and the third structural mode in the in-line direction with a 2:1 (in-line:cross-flow) ratio between structural mode frequencies. Since it was found with cylinder 2 that an asymmetric second mode could not be excited under the experimental conditions, it was hypothesized that by tuning the in-line direction to be excited with a higher odd mode shape, the system may respond with an excitation of the higher odd mode. An analytic model of the structural characteristics for cylinder 3 indicated that the cylinder would pass through several modes up to the fourth structural mode in-line while still encountering a range of frequencies close to the first mode in the cross-flow direction.

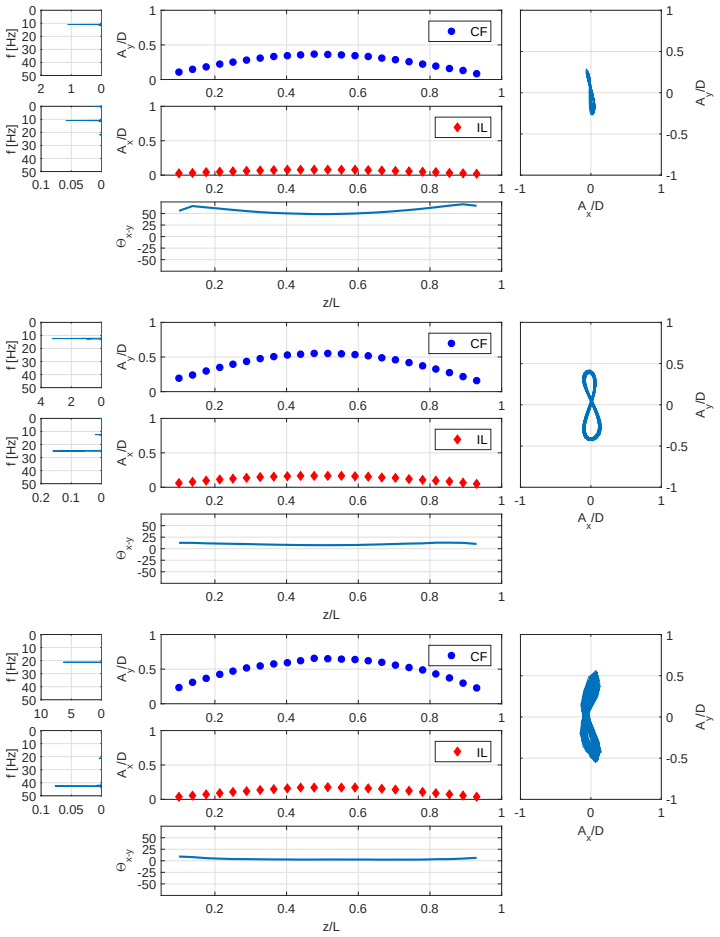

Figure 8: Spanwise response of cylinder 3, showing the frequency spectrum for the center point in cross-flow and in-line directions, the phase averaged maximum spanwise response in the cross-flow and in-line directions, the computed phase between in-line and cross-flow motions, and the Lissajous figure of the center point. Top image: Vr_n = 7.3. Middle image: Vr_n = 8.4. Bottom image:Vr_n = 14.1.

Figure 8 shows the spanwise response of cylinder 3 at three different normalized reduced velocity values, V_{rn} = 7.3, V_{rn} = 8.4, and V_{rn} = 14.1. The lowest reduced velocity is in a region, as indicated by Fig. 5, where the response frequency in the in-line direction is equal to the frequency in the cross-flow direction. The other two cases show the

response just after the dominant frequency in the in-line direction switches to be twice the cross-flow frequency. The last test case shows the response at the highest reduced velocity tested to demonstrate how the response changes with an increase in reduced velocity.

The top image of Fig. 8 shows the response at $V_{rn} = 7.3$ where the dominant in-line and cross-flow response frequencies are equal. The Lissajous figure in this case shows a squished tear drop shape response, where the in-line motion is slightly larger at the bottom of the orbit than at the top. This type of asymmetric response has been observed previously in experiments on elastically mounted rigid cylinders, where the in-line natural frequency is tuned to have a frequency lower than the cross-flow natural frequency (Kang and Jia, 2013). Based on the natural frequencies of the cylinder in the in-line direction, the frequency of oscillation for this test case ends up being closest to the second mode frequency in the in-line direction, which is equal to the first mode frequency in the cross-flow direction. This results in a response with frequencies being the same in both directions, although the second spanwise mode shape is not excited in the in-line direction. Instead, similar to cylinder 2, the spanwise in-line response resembles a half sine shape (although with only very small amplitude motion in the in-line direction).

The middle image in Fig. 8 shows the spanwise response of cylinder 3 at nominal reduced velocity of 8.4 where the cylinder has transitioned to oscillate with a 2:1(in-line:cross-flow) frequency relation. Figure 5 shows that cylinder oscillates with a frequency close to the third mode in the in-line direction and a frequency close to the first mode in the cross-flow direction at this reduced velocity. Similar to cylinder 2, the expected frequency relation is achieved in exciting the response of the cylinder, but again, the spanwise response of the cylinder does not follow the structural mode shape if the system were undergoing resonance at these frequencies. The cylinder again displays a spanwise shape similar to a half sine in both the in-line and cross-flow directions, rather than having a third mode shape in the in-line direction.

The bottom image in Fig.8 shows the spanwise response of cylinder 3 at nominal reduced velocity of 14.1. This case is similar to the previous case, demonstrating a 2:1 frequency relation between the in-line and cross-flow motion, but a half sinusoid spanwise shape. The resulting cross-flow frequency for this reduced velocity is directly between the first and second mode frequencies of the structure. If higher flow speed tests were possible with this setup, it is anticipated that the second mode of the structure in the cross-flow direction would be excited with the fifth mode in-line being the closest structural mode to the in-line excitation frequency.

With the relatively short span cylinder tested and optical motion tracking techniques, higher mode excitation of the cylinder is not observable by simply observing the spanwise response. Additionally, due to the nonlinear coupling of the fluid and structure, it is difficult to quantify particular modes being excited based simply on the structural modes of the cylinder, so multivariate analysis techniques are employed later to quantify the empirical modes excited in the structure.

4.1.4. Cylinder 4 - Tensioned cylinder

Figure 9 shows the spanwise response of cylinder 4 for increasing flow speeds as in Gedikli and Dahl (2017). The top image in Figure 9 shows the response at $V_{rn} = 10.6$ and bottom image shows the response at $V_{rn} = 18.1$. These two reduced velocity values were selected based on the frequency response shown in Fig.5, where at $V_{rn} = 10.6$, the test cylinder oscillates with two dominant frequencies in both the in-line and cross-flow directions. The multiple dominant frequencies observed for this case are the same in both the in-line and cross-flow directions and are partly a function of the slight asymmetry in the response of the cylinder, as evident in the Lissajous figure. The spanwise response in both in-line and cross-flow directions demonstrate a first mode shape based on observation of the magnitude of the spanwise response, although some asymmetry does exist over the span. Since the dominant frequencies at these flow speeds lie closest to the first mode of the structure in the cross-flow direction, it is expected that the spanwise shape in the cross-flow direction resembles a first mode, however, similar to cylinder 2, the frequency in the in-line direction lies closest to the second mode, yet the spanwise shape does not strongly demonstrate a second mode shape.

The bottom image in Fig.9 shows the spanwise response for cylinder 4 at $V_{rn} = 18.1$. At this flow speed, the excitation frequency in the cross-flow direction is close to the second mode structural natural frequency and the response in the cross-flow direction has changed to resemble a second mode shape in the cross-flow direction. The response in the in-line direction appears to have second and third mode components based on the shape of the response, despite a single dominant frequency for the response. Multivariate analysis is used to further elucidate the modal excitation of the structure based on empirical modes.

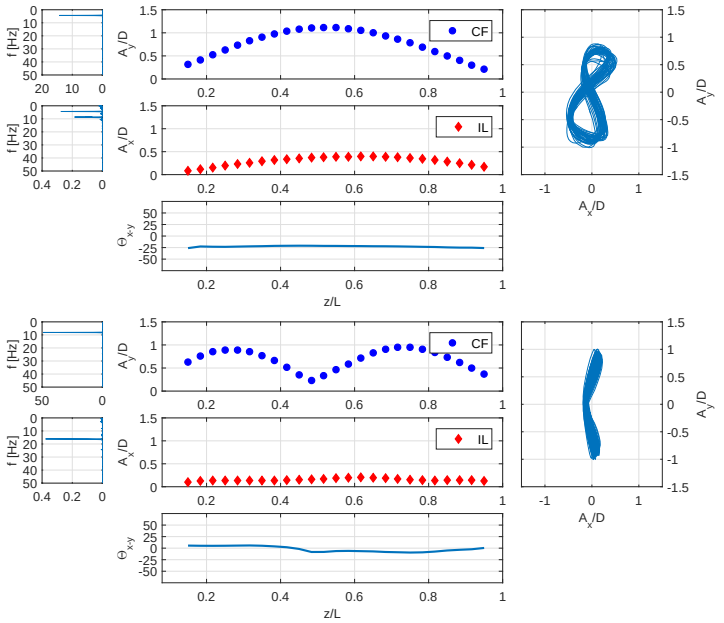

Figure 9: Spanwise response of cylinder 4, showing the frequency spectrum for the center point in cross-flow and in-line directions, the maximum spanwise response in the cross-flow and in-line directions, the computed phase between in-line and cross-flow motions, and the Lissajous figure of the center point. Top image: $Vr_n = 10.6$. Bottom image:$Vr_n = 18.1$.

One important observation from all the cylinders tested, is that even though the cylinder has a frequency that may correspond to a higher structural mode in the in-line direction (second mode for example), if there is no change in the cross-flow spanwise mode as flow speed is increased or if the response of the structure is at a frequency that is closest to the first mode frequency, there is no observed spanwise mode shape change in the in-line direction. For example, as with cylinder 4, a change in the shape of the in-line direction response is only observed after the cross-flow motion has undergone a spanwise mode shape change due to excitation of a higher structural mode. These results are only observed for the low mode number flexible cylinders that are tested in the current experiments, however care has been taken to maintain a uniform current and uniform loading of the structure in the flow channel by performing the experiments horizontally in the flow channel. Vertical orientation of the cylinder could introduce asymmetries to the loading through gravitational effects or effects of the free surface.

In addition to higher modes in the in-line direction being delayed based on the mode excitation in the cross-flow direction, the present experiments show that it is difficult to excite asymmetric mode shapes in the in-line direction under a uniform current loading, although asymmetric mode shapes can be excited in the cross-flow direction. It is not possible to claim that this observation is true under all flow conditions, especially since slight asymmetries to an experiment or typical asymmetries that may exist in a field experiment could possibly excite asymmetric modes.

These findings are based primarily on analysis of the observed maximum response over the span. In order to further understand which dominant modes are excited, particularly in the in-line direction, it is necessary to decompose the observed responses into dominant empirical modes to clearly see the contribution of each mode in the total response. Empirical modes are chosen to characterize the spanwise response of the cylinders in order to avoid requiring particular mode shapes for a phenomenon that is well known to be nonlinear. For this purpose, the recently developed smooth orthogonal decomposition (SOD) (Gedikli et al., 2017) is used to characterize the modal response of the different cylinders.

5. Multivariate analysis - SOD based VIV mode analysis

Proper orthogonal decomposition (POD) has been widely used in structural vibration modal identification and is shown to converge to the actual vibration modes if the mass distribution in the linear dynamical systems is uniform

(i.e., when structural modes form an orthogonal basis for the linear system's phase space) as shown by Feeny and Kappagantu (1998). Alternatively, if the actual mass matrix is known, POD can identify the true vibration modes by premultiplying the motion data by the mass matrix. Due to the uniform distribution of the measurement dots along the beam, the mass distribution of the corresponding discrete system is expected to be uniform in the air (i.e., one expects a uniform diagonal mass matrix). However, when placed in a fluid, the mass matrix is no longer uniform or constant due to the spanwise added mass, and the structural modes are no longer expected to form an orthogonal basis. In contrast, Chelidze and Zhou (2006) showed that smooth orthogonal decomposition (SOD) does not require the knowledge of mass distribution to converge to the actual vibration modes and is expected to be better at resolving structural modes responsible for this type of fluid structure interaction.

The main difference of such multivariate methods than traditional Fourier based mode decomposition is that Fourier based mode decomposition assumes a base modal shape. The empirical multivariate methods used in the present paper do not require any prior knowledge of the mode shape as an input parameter. The resulting empirically determined mode shapes may be similar to a sinusoidal mode shape depending on the loading of the cylinder and for highly non-linear systems, such as low mode number flexible cylinders with multiple excited modes, these methods can be advantageous for identifying the dominant empirical modes.

Previously, Gedikli and Dahl (2017) applied local POD analysis and Gedikli et al. (2017) applied global POD and SOD to a similar VIV dataset, comparing the results of these two techniques on the analysis of a flexible cylinder undergoing VIV. In the local analysis, the POD method was applied to individual cylinder responses to obtain empirical mode shapes for each individual reduced velocity. In the global analysis, the method is applied to all cylinder time histories over all reduced velocities, creating one large input data matrix, to obtain a single global response describing the system modes. The global analysis method effectively determines an average modal behavior of the system over the measurements in the data set. In both studies, the methods identified the cylinder's most dominant empirically determined mode shapes; however, Gedikli et al. (2017) showed that by applying the global SOD method, the proper ordering of empirical modes based on energy content could be achieved. Therefore, in this study we use the global SOD method for empirical modal analysis of the cylinders.

5.1. Description of smooth orthogonal decomposition (SOD)

In the SOD method, the displacement data matrix, X, is constructed from all the experimentally measured time histories from the cross-flow and in-line measurements. $X \in R^{m\times 2n}$, where X is the combined in-line and cross-flow data matrix, m is the number of total time samples, and n is the number of points recorded along the span of the cylinder. Using the forward difference method, one can construct a new data matrix $V = DX \in R^{m\times 2n}$ which includes in-line and cross-flow velocities. With the new velocity data matrix, the phase space representation of the total response can be obtained as $Y = [X, V] \in R^{n\times 4n}$.

SOD identifies the subspaces (ψ) where the scalar field projection $q = Y\psi$ is maximally smooth, while having maximal variance. Defining the smoothness of the projection as

$$h(\psi; k) = \frac{1}{M}(D^k Y\psi)^T D^k Y\psi \tag{4}$$

where D^k is the k^{th} order derivative matrix based on forward difference ($k = 3$ for this application), SOD translates into the following optimization problem:

$$\max_{\psi} q(\psi)^T q(\psi) = \max_{\psi} (Y\psi)^T Y\psi, \tag{5}$$

subject to

$$\min_{\psi} \left(D^k q(\psi)\right)^T D^k q(\psi) = \min_{\psi} \left(D^k Y\psi\right)^T D^k Y\psi\,. \tag{6}$$

The corresponding SOD problem can be solved by generalized singular value decomposition:

$$Y = UC\Phi^T = Q\Phi^T, \quad D^k Y = ZS\Phi^T = D^k Q\Phi^T\,, \tag{7}$$

where U and Z are unitary matrices; C and S are diagonal matrices; columns of the square matrix Φ contain smooth orthogonal modes (SOMs); columns of $Q = UC$ are smooth orthogonal coordinates (SOCs); $\lambda_i = C_{ii}/S_{ii}$ are smooth

orthogonal values (SOVs); and $\Psi = \Phi^{-T}$ are smooth projective modes (SPMs) that form a bi-orthogonal set with SOMs.

5.2. Energy contribution and empirical VIV modes

It was identified previously that the response of the system in the in-line direction appears to be driven by the response of the system in the cross-flow direction. When there is a uniform in-flow distributed over the span of the cylinder, the dominant shape of the in-line response tended to remain a half sine shape unless the cross-flow mode shape changed, in which case, the in-line response would display a combination of higher mode shapes. This phenomenon is investigated further by employing an empirical modal analysis to the cylinder 2 and cylinder 4 datasets. These data sets are chosen since they both have frequency characteristics such that the second structural mode in the in-line direction is tuned to have twice the frequency of the first mode in the cross-flow direction, although cylinder 2 is bending dominated and cylinder 4 is tension dominated.

In order to assess the dominant empirical modes present in the data set, the data for each cylinder is split into subsets over which the smooth orthogonal decomposition is applied. For cylinder 2, the mode shapes are calculated using flow speeds corresponding to excitation frequencies below the natural frequency of the cylinder ($V_{rn} < 5.5$, labeled as (a) in Figure 10) and for flow speeds corresponding to excitation frequencies above the natural frequency of the cylinder ($V_{rn} > 5.5$, labeled as (b) in Figure 10). The global SOD analysis is separately performed over these ranges of experiments. The choice of separating the data based on the cylinder natural frequency is somewhat arbitrary, but it allows one to see how the dominant empirical mode behavior changes if one is observing the system excitation below the first structural mode frequency and above the first structural mode frequency (where the system may be approaching excitation of the second structural mode). In this way, one can compare the ordering of dominant modes present and one may observe if how different modes become dominant over different ranges of data.

Similarly, the data set for cylinder 4 is divided into two parts for computing the SOD. For cylinder 4, the data is divided into speeds for $V_{rn} < 15$ (labeled (a) in Figure 11) and speeds for $V_{rn} > 15$ (labeled (b) in Figure 11). This dividing point is chosen since the system is observed to undergo a mode change in the cross-flow direction at this speed, hence the lower speeds correspond to a dominant half-sine-like excitation in cross-flow and the higher speeds correspond to a dominant full-sine-like excitation in cross-flow.

In applying the SOD method, the separately measured in-line and cross-flow responses are used in computing the mode shapes, hence each mode shape consists of a cross-flow portion and an in-line portion. The SOD method also allows for computation of the frequency associated with each mode. In the global SOD method, the resulting frequency corresponds to an average dominant frequency over the range of experiments used in computing the mode shapes. These average frequencies are given in Figures 10 and 11 for each mode shape to illustrate the average frequency associated with that modal response of the cylinder. In some cases, there are multiple dominant frequencies for a single mode (for example, if a mode is composed of both a significant in-line response and a significant cross-flow response where each direction has a different dominant frequency), then multiple dominant frequencies are reported.

Figure 10(i) shows the energy fraction of the first 10 subspace dimensions from SOD along with the corresponding frequencies for the first 6 dominant smooth orthogonal modes of cylinder 2. As previously described, the energy fraction labeled as (a) shows the modal components for low speeds (below $V_{rn} = 5.5$), while the line labeled as (b) shows the same computation using speeds higher than $V_{rn} = 5.5$. It is immediately apparent that in either decomposition of the response, the majority of energy is comprised by the first four empirical modes. Figure 10(ii) shows the first six smooth orthogonal modes for the lower speed (a) data set and Figure 10(iii) shows the first six smooth orthogonal modes for the higher speed (b) data set. Since the first four modes contain the majority of energy in the system, one only needs to consider these modes. The first two modes correspond to a pure cross-flow motion of the system with the associated average frequency, this shape is consistent with what one might consider the expected first mode structural response of the system. The third and fourth modes for group (a) (Figure 10(ii)) correspond to a purely in-line response of the system with a half-sine-like shape and twice the frequency of the pure cross-flow modes. For the higher flow speeds, group (b) (Figure Figure 10(iii)), the first two modes are very similar. The higher frequency of these modes corresponds to the higher excitation frequencies at the higher flow speed. The third mode, however shows a pure cross-flow, full-sine-like shape, which demonstrates that the system may be near to transitioning to exciting a second mode in the cross-flow direction (i.e. some of the higher flow speed experiments had sufficient responses containing some second mode excitation in order to reorder the empirical modes based on the system velocity rather than just energy content, an effect of using the SOD method). From the low speed data, the closest empirical mode

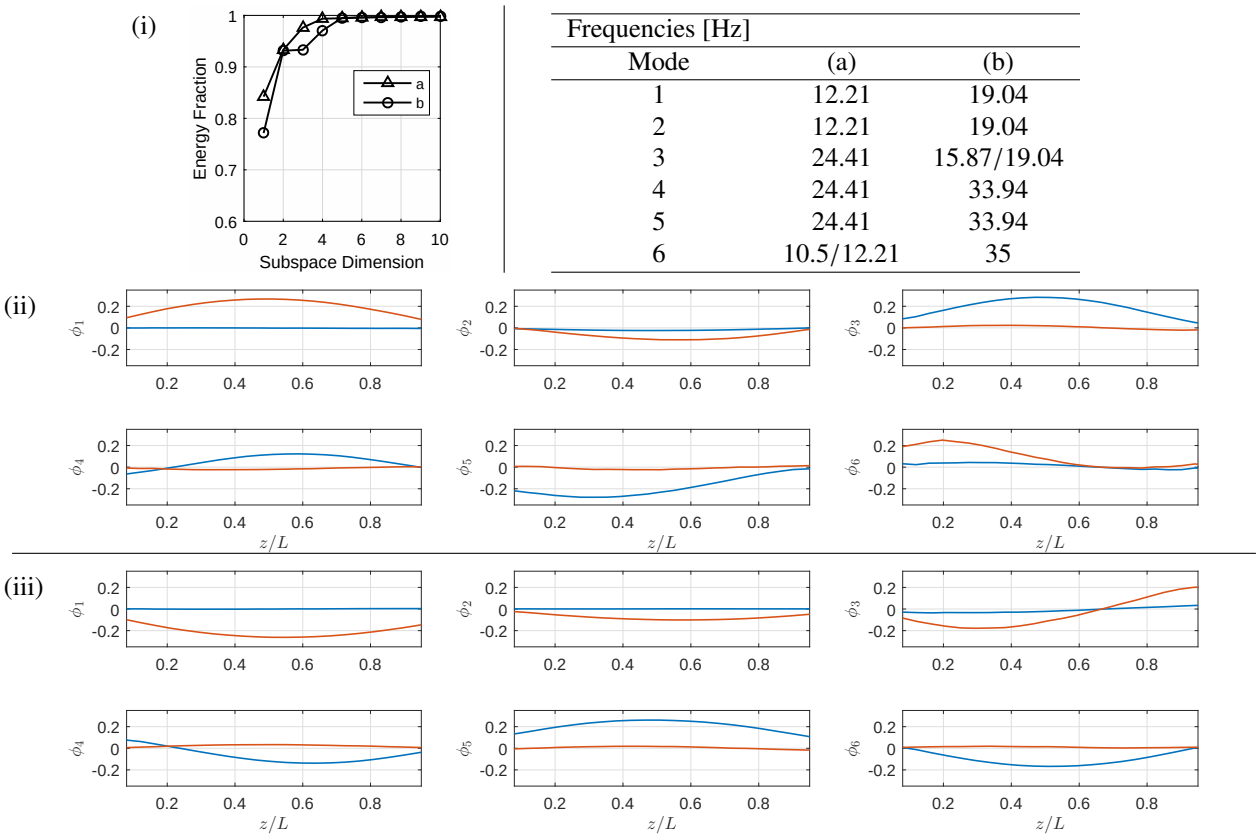

Frequencies [Hz]		
Mode	(a)	(b)
1	12.21	19.04
2	12.21	19.04
3	24.41	15.87/19.04
4	24.41	33.94
5	24.41	33.94
6	10.5/12.21	35

Figure 10: (i) Energy fraction in first 10 subspace dimension, (ii) First 6 SOMs for cylinder 2 where input data matrix includes the dataset up to $V_{rn} = 5.5$. (iii) First 6 SOMs for cylinder 2 where input data matrix includes dataset after $V_{rn} = 5.5$. Red is cross-flow, blue is in-line.

corresponding to this type of shape was mode 6. Mode 4 in group (b) is similar to mode 4 in group (a), while mode 5 from group (b) corresponds with mode 3 from group (a). The same modes appear to be present, but are just reordered based on the smoothness of the decomposition. The main thing to note from these decompositions is that the dominant in-line modes (mode 3 and 4 in group (a), and modes 4 and 5 in group (b)) remain with a half sine shape when the dominant cross-flow modes have a half sine shape (modes 1 and 2 in both groups). Despite the frequencies of the in-line modes corresponding to frequencies close to the structural second mode frequency, the shape of these modes remains symmetric, corresponding to the shape of the dominant cross-flow mode. Unfortunately, due to limitations of the experimental setup, the flow speed could not further be increased, where it would be expected that the second structural mode in the corss-flow direction would be excited. This is due to the frequency relation of the bending dominated system. For cylinder, 4, it was possible to have a system with a larger range of modes covered by the allowable range of speeds in the flow channel.

Figure 11(i) shows the energy fraction of the first 10 subspace dimensions from SOD along with the corresponding frequencies for the first 6 dominant smooth orthogonal modes of cylinder 4. Again, as previously described, the energy fraction labeled as (a) shows the modal components for speeds below the cross-flow mode transition (below $V_{rn} = 15$), while the line labeled as (b) shows the same computation using higher speeds after the mode transition at $V_{rn} = 15$. In group (a), the energy content of the modes is largely present in the first three modes, which as seen in Figure 11(ii), correspond to a pure cross-flow excitation with half sine shape (mode 1), a pure cross-flow excitation with full sine shape (mode 2), and a combined in-line and cross-flow excitation with half sine shape with separate dominant frequencies for each direction (mode 3). In contrast, the energy is distributed over the first 6 modes for group (b), and as seen in Figure 11(iii), these modes contain more complex behaviors consisting of multiple frequencies and complicated mode shapes. In group (b), the dominant mode is a pure cross-flow mode with full sine shape, similar

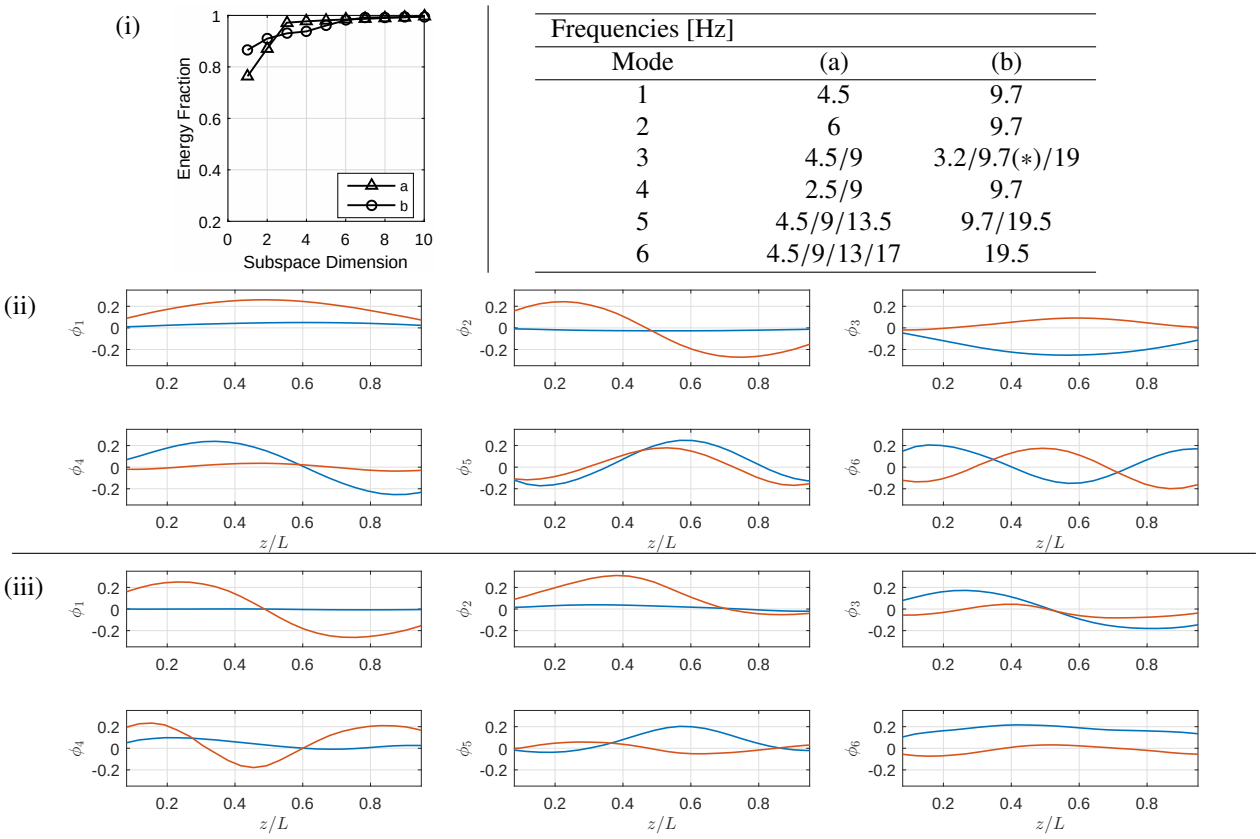

Frequencies [Hz]		
Mode	(a)	(b)
1	4.5	9.7
2	6	9.7
3	4.5/9	3.2/9.7(∗)/19
4	2.5/9	9.7
5	4.5/9/13.5	9.7/19.5
6	4.5/9/13/17	19.5

Figure 11: (i) Energy fraction in first 10 subspace dimension, (ii) First 6 SOMs for cylinder 4 where input data matrix includes the dataset up to $V_{rn} = 15$. (iii) First 6 SOMs for cylinder 4 where input data matrix includes dataset after $V_{rn} = 15$. Red is cross-flow, blue is in-line.(*) is the most dominant frequency.

to the second structural mode in the cross-flow direction. In this case, the transition of the dominant mode to be the second structural mode in the cross-flow direction enables the system to display more complex mode behavior in the in-line direction. For example, mode 3 of group (b) shows a full sine shape and mode 5 displays a shape similar to a third mode. This multimodal excitation of the in-line direction is only observed once the system has transitioned between exciting the first cross-flow structural mode to the second cross-flow structural mode.

It must be noted that any analysis of a system using empirical modes is subject to flaws in the data acquisition and available data and will always be difficult to interpret in terms of general behaviors for any similar system. It is only our intention in this analysis to demonstrate how the dominant in-line modes change as a function of the dominant cross-flow mode, since analysis of the raw amplitude response cannot give information about individual modes. One can argue from this set that by observing similar behaviors in the separate bending-dominated and tension-dominated systems, one may expect similar behaviors in systems with combined bending and tension.

6. Discussion

The cylinders studied in this experiment were designed specifically with the intention of exciting specific spanwise mode shapes in order to study the effects of the spanwise response of the cylinder on VIV. By keeping the ratio of natural frequencies between the in-line and cross-flow direction to be 2:1 while altering the structural mode shapes associated with these frequencies, it was hypothesized that a different system response would be observed. In these experiments, it was observed that in a uniform flow, when the excitation frequency from vortex shedding matches the in-line natural frequency and that natural frequency corresponds to an asymmetric mode (2nd mode in this case), the response will not take on the asymmetric mode shape but will still be excited with the twice the cross-flow frequency.

Vandiver and Jong (1987) observed a similar behavior in field experiments where excitation of specific odd mode frequencies in the in-line direction were observed to take on a lower mode shape. This behavior was attributed to the symmetric distribution of the drag force over the cylinder in a uniform flow, where due to the symmetry of loading over the body, the forced oscillation would not allow for even modes to be excited. Consider the classical problem of a viscously damped Euler-Bernoulli beam with pinned end conditions (Benaroya, 2004; Ginsberg, 2001; Meirovitch, 2001). If one considers a uniform distribution of force over the span of the beam (consider this to be the uniformly distributed drag force acting in the in-line direction of the cylinder), where the force is a harmonic function applied with a frequency equal to the second mode natural frequency, one finds that the spanwise response will have a symmetric shape similar to the shape observed in the present experiments (see Fig. 12). In fact, for any frequency associated with an even mode, the spanwise response will be similar to the next lowest odd mode shape. This is a well known phenomenon based on the modal analysis of beams, however the nonlinear coupling between the in-line and cross-flow response of the flexible cylinder undergoing VIV leads to additional behaviors that are not predicted by this simple dynamic beam theory.

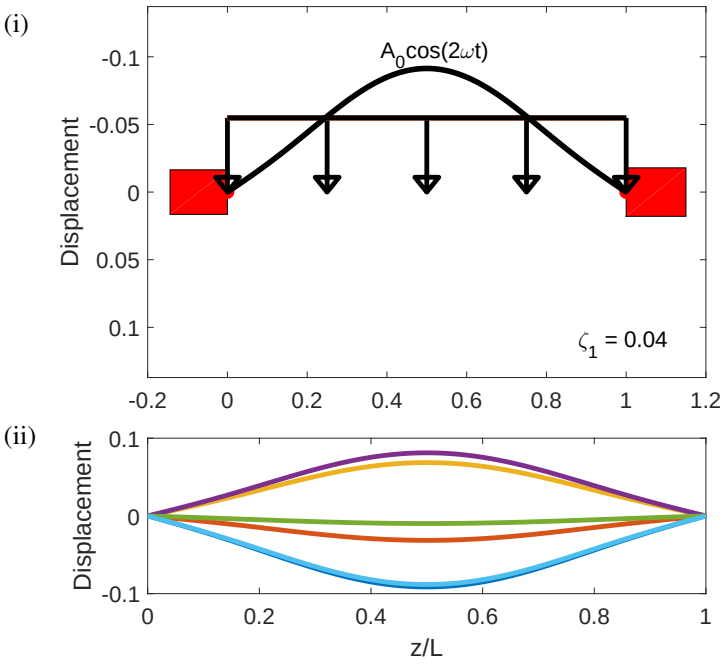

Figure 12: Euler-Bernoulli beam with uniformly distributed, time dependent load with frequency equal to the second mode structural natural frequency.Top image (i): Schematic of load distribution and resulting maximum structure spanwise response. Bottom image (ii): Structural response at different instances in time.

If one considers a beam where the uniformly distributed forcing function is applied with a frequency equal to the third mode of the cylinder, one will find that although the distribution of the force does not match the mode shape for that frequency, the beam will still respond with a spanwise response that resembles the third mode shape (see Figure 13. The response amplitudes may not be as large as would happen if the distribution of the load followed the third mode shape, but the spanwise response still takes this shape when we consider only loading in one direction. In the case of the present experiments, there is a combined loading on the cylinder in both the cross-flow and in-line directions due to vortex shedding in the wake of the cylinder. This combined load sets up an effective resonant condition in the cross-flow direction, where the added mass of the system adjusts the effective natural frequency. Dahl et al. (2010) found that for an elastically mounted rigid cylinder, the in-line added mass would adjust as well in order to provide an effective resonant condition in the in-line direction. However, even when the in-line forcing frequency matches the in-line natural frequency for a higher mode shape other than the cross-flow mode, as with cylinder 2 and 3, the in-line response is dominated by a half sine shape. This is observed to happen due to the half sine shape that dominates the cross-flow response. This makes sense since the forcing functions applied in the cross-flow and

in-line directions are derived from the same physical phenomenon, the shedding of vortices in the wake, which causes the responses in the separate directions to be coupled. One therefore can't separately consider the in-line response from the cross-flow response, otherwise the resulting spanwise mode shape would be predicted incorrectly. Once the cross-flow mode shifts to exciting a higher mode shape in the cross-flow direction, then one begins to see higher mode responses in the in-line direction.

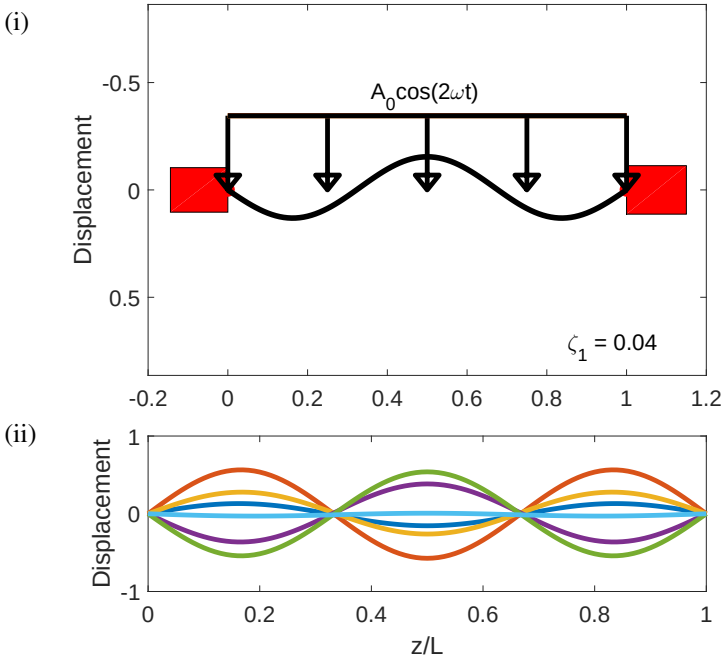

Figure 13: Euler-Bernoulli beam with uniformly distributed, time dependent load with frequency equal to the third mode structural natural frequency.Top image (i): Schematic of load distribution and resulting maximum structure spanwise response. Bottom image (ii): Structural response at different instances in time.

Although the observed in-line responses did not demonstrate strong even mode excitation in these experiments, even modes could certainly be excited in the case of sheared flow, where an asymmetry of the flow speed would result in an asymmetry to the distributed drag load. This may also be significant to flexible cylinder studies conducted vertically in a towing tank or water tunnel. In conditions where a flexible cylinder pierces the water surface, a slight asymmetry may occur in the loading of the structure due to the formation of waves at the free surface, which would demonstrate asymmetric mode excitation that would not typically occur if the loading was purely symmetric. This has general relevance in understanding responses observed in field or lab experiments studying the response of flexible cylinders.

Additional interesting behaviors were also observed for specific cylinders. For example, cylinder 3 was tuned so that the first mode in-line would correspond with the forcing frequency from vortex shedding in the transverse direction, while the third structural mode will correspond with the vortex shedding frequency in the in-line direction. Despite this tuning, the in-line direction undergoes a response with dominant first mode shape (due to the loading distribution as described above). This is interesting, however, since in order to oscillate with the observed frequency and mode, a linear treatment of the frequency response and adjustment of the effective natural frequency would require an extremely large negative added mass, since the frequency of oscillation in the in-line direction is so far from the natural frequency associated with the first mode. This is highly unlikely and the frequency transitions observed for cylinder 3 are more likely to stem from non-linear resonant conditions from the coupling of vortex shedding effects on the cross-flow and in-line response. Additionally, the transition of the cross-flow response of cylinder 4 from first mode to second mode, that leads to a multi-mode response in the in-line direction implies that the in-line response is a forced response dependent on the cross-flow response. Further studies to investigate the three-dimensional wake in the presence of these transitions would help in understanding the importance of these couplings and would aid in

developing improved physical models of the wake for prediction of this phenomenon.

Finally, the transition between a 1:1 mode shape response and 2:3 mode shape response seen in the tensioned cylinder is not necessarily unique to the tensioned cylinder, since the natural frequency relation for the bending-dominated cylinder requires the natural frequencies to be further spaced from one another. Due to the limitations of the flow channel, higher speeds could not be tested to see if the transition to higher modes would follow a similar behavior for the bending-dominated systems.

The tension-dominated and bending-dominated systems in this study demonstrate some overall common behaviors: despite frequency excitation in the cross-flow direction that is twice the frequency in the in-line direction and tuning natural frequencies to have specific mode shapes, it is difficult or not possible to significantly excite an asymmetric second mode shape in the in-line direction. There are several stipulations on this observation: 1) This phenomenon is limited to occur only under symmetric loading conditions (i.e. uniform loading), which are likely rarely seen in field operations, 2) the cylinder has to have a symmetric mass distribution, otherwise variation in the mass could result in system asymmetries, 3) in the present experiments, the mass ratio was small (close to 1), such that gravitational effects on the structure (i.e natural sagging of the cylinder) were minimal, and 4) the orientations of the test cylinders were always horizontal, hence small asymmetries that may occur by having the cylinder vertical are avoided (e.g. piercing through the free surface).

7. Conclusion

The objective of this experimental study was to observer the effects of a flexible cylinder's structural mode shapes on its response due to vortex-induced vibrations. Previously in field experiments, Vandiver and Jong (1987) observed that a flexible pipe would not be excited with even modes due to a uniformly distributed drag load along the span. This study tests this observation in controlled laboratory experiments and further investigates the effects of exciting specific mode shape combinations in the structure by systematically altering the cylinder structural characteristics using plastic beams molded inside flexible urethane cylinders. Each of the test cylinders had unique structural characteristics allowing the in-line mode shape to vary from one to three while keeping the cross-flow mode shape and ratio between the in-line and cross-flow frequencies 2:1.

This systematic study shows that even though a flexible cylinder may be tuned to oscillate with an asymmetric mode shape (i.e. second mode) in in-line, it is not possible to have an asymmetric mode shape due to symmetric drag loading in a uniform flow. Further, it is not possible to excite higher mode shapes in the in-line direction without a transition to a higher mode shape in the cross-flow direction. Asymmetric mode shapes may be possible if the drag force distribution is not symmetric. Multivariate analysis was used to analyze the contribution of higher order empirical modes, demonstrating how higher modes in the in-line direction become dominant after a mode transition in the cross-flow direction.

Further work is necessary to elucidate how general this behavior is in long flexible cylinders. Due to the relatively short aspect ratio of the cylinders and uniform flow in the present study, significant traveling wave responses on the cylinder were not observed, which would alter the generality of these observations. Additionally, three-dimensional visualization of the wake would help to quantify the fluid-structure coupling over the span as mode transitions occur.

References

Bearman, P., 2011. Circular cylinder wakes and vortex-induced vibrations. Journal of Fluids and Structures 27, 648–658.

Bearman, P.W., 1984. Vortex shedding from oscillating bluff bodies. Annual review of fluid mechanics 16, 195–222.

Benaroya, H., 2004. Mechanical Vibration: Analysis, Uncertainties, and Control. 2 ed., Marcel Dekker, New York.

Chaplin, J., Bearman, P., Huarte, F.H., Pattenden, R., 2005. Laboratory measurements of vortex-induced vibrations of a vertical tension riser in a stepped current. Journal of Fluids and Structures 21, 3–24.

Chelidze, D., Zhou, W., 2006. Smooth orthogonal decomposition-based vibration mode identification. Journal of Sound and Vibration 292, 461 – 473. URL: http://www.sciencedirect.com/science/article/pii/S0022460X05005948, doi:http://doi.org/10.1016/j.jsv.2005.08.006.

Dahl, J., Hover, F., Triantafyllou, M., 2006. Two-degree-of-freedom vortex-induced vibrations using a force assisted apparatus. Journal of Fluids and Structures 22, 807–818.

Dahl, J., Hover, F., Triantafyllou, M., Dong, S., Karniadakis, G., 2007. Resonant vibrations of bluff bodies cause multi-vortex shedding. Physical Review Letters 99.

Dahl, J., Hover, F., Triantafyllou, M., Oakley, O., 2010. Dual resonance in vortex-induced vibrations at subcritical and supercritical reynolds numbers. Journal of Fluid Mechanics 643, 395–424.

Feeny, B., Kappagantu, R., 1998. On the physical interpretation of proper orthogonal modes in vibrations. Journal of Sound and Vibration 211, 607 – 616. URL: http://www.sciencedirect.com/science/article/pii/S0022460X97913869, doi:http://dx.doi.org/10.1006/jsvi.1997.1386.

Gedikli, E.D., Dahl, J.M., 2017. Mode excitation hysteresis of a flexible cylinder undergoing vortex-induced vibrations. Journal of Fluids and Structures 69, 308 – 322. URL: http://www.sciencedirect.com/science/article/pii/S0889974616303188, doi:http://dx.doi.org/10.1016/j.jfluidstructs.2017.01.006.

Gedikli, E.D., Dahl, J.M., Chelidze, D., 2017. Multivariate analysis of vortex-induced vibrations in a tensioned cylinder reveal nonlinear modal interactions, in: 10th International Conference on Structural Dynamics, Eurodyn.

Ginsberg, J., 2001. Mechanical and Structural Vibrations: Theory and Applications. John Wiley and Sons.

Huera-Huarte, F., Bangash, Z., González, L., 2014. Towing tank experiments on the vortex-induced vibrations of low mass ratio long flexible cylinders. Journal of Fluids and Structures 48, 81–92.

Kang, Z., Jia, L., 2013. An experiment study of a cylinder's two degree of freedom viv trajectories. Ocean Engineering 70, 129–140.

Lie, H., Kaasen, K., 2006. Modal analysis of measurements from a large-scale {VIV} model test of a riser in linearly sheared flow. Journal of Fluids and Structures 22, 557 – 575. URL: http://www.sciencedirect.com/science/article/pii/S0889974606000077, doi:http://dx.doi.org/10.1016/j.jfluidstructs.2006.01.002.

Marcollo, H., Eassom, A., Fontaine, E., Tognarelli, M., Beynet, P., Constantinides, Y., Oakley, O.H., 2011. Traveling wave response in full-scale drilling riser viv measurements, in: ASME 2011 30th International Conference on Ocean, Offshore and Arctic Engineering, American Society of Mechanical Engineers. pp. 523–537.

Meirovitch, L., 2001. Fundamentals of Vibrations. McGraw-Hill, New York, NY.

Modarres-Sadeghi, Y., Chasparis, F., Triantafyllou, M., Tognarelli, M., Beynet, P., 2011. Chaotic response is a generic feature of vortex-induced vibrations of flexible risers. Journal of Sound and Vibration 330, 2565–2579.

Passano, E., Larsen, C.M., Wu, J., 2010. Viv of free spanning pipelines: Comparison of response from semi-empirical code to model tests, in: ASME 2010 29th International Conference on Ocean, Offshore and Arctic Engineering, American Society of Mechanical Engineers. pp. 567–577.

Sarpkaya, T., 2004. A critical review of the intrinsic nature of vortex-induced vibrations. Journal of Fluids and Structures 19, 389–447.

Sarpkaya, T.S., 2010. Wave Forces on Offshore Structures. Cambridge University Press. doi:10.1017/CBO9781139195898.009.

Srinil, N., Zanganeh, H., Day, A., 2013. Two-degree-of-freedom viv of circular cylinder with variable natural frequency ratio: Experimental and numerical investigations. Ocean Engineering 73, 179–194.

Trim, A., Braaten, H., Lie, H., Tognarelli, M., 2005. Experimental investigation of vortex-induced vibration of long marine risers. Journal of fluids and structures 21, 335–361.

Vandiver, J., Jong, J.Y., 1987. The relationship between in-line and cross-flow vortex-induced vibration of cylinders. Journal of Fluids and Structures 1, 381–399.

Vandiver, J., Marcollo, H., Swithenbank, S., Jhingran, V., et al., 2005. High mode number vortex-induced vibration field experiments, in: Offshore Technology Conference, Offshore Technology Conference.

Williamson, C., Govardhan, R., 2004. Vortex-induced vibrations. Annu. Rev. Fluid Mech. 36, 413–455.